Cite this: DOI: 10.1039/c0xx00000x

www.rsc.org/xxxxxx

ARTICLE TYPE

Crystal form selectivity by humidity control: the case of the ionic co-crystals of nicotinamide and $CaCl_2$

Dario Braga,[a] Fabrizia Grepioni,[a] Giulio I. Lampronti,*[b] Lucia Maini,*[a] Katia Rubini,[a] Federico Zorzi,[c] Alessandro Turrina[d]

Received (in XXX, XXX) Xth XXXXXXXXX 20XX, Accepted Xth XXXXXXXXX 20XX
DOI: 10.1039/b000000x

Post-synthesis (de)hydration techniques are here used to explore further hydrated forms of ionic co-crystals (ICCs) of nicotinamide with $CaCl_2$. Humidity is shown to be a crucial factor for ICCs, which cannot be ignored for a complete polymorph screening in this class of compounds. The exposure of nicotinamide·$CaCl_2$·H_2O obtained by kneading reaction to controlled relative humidity of 75% leads to the formation of a new hydrated phase: nicotinamide·$CaCl_2$·$4H_2O$. When nicotinamide·$CaCl_2$·H_2O is exposed to a relative humidity between 32% and 54%, nicotinamide$_2$·$CaCl_2$·$2H_2O$ was obtained. The anhydrous form was achieved in the result of overnight dehydration of nicotinamide·$CaCl_2$·H_2O at 150 °C. The tetrahydrated form cannot be obtained as first product for kinetic (or thermodynamic) reasons. Control of the relative humidity has proven to be an efficient way to selectively isolate and stabilize powders of pure hydrous ICC phases, which is fundamental for industrial applications. Crystalline structures of nicotinamide·$CaCl_2$·$4H_2O$ and anhydrous nicotinamide·$CaCl_2$ were determined from powder diffraction.

Introduction

The design of new molecular co-crystals has in recent years received a growing interest from fields where the final product is used and commercialized as a solid phase especially the pharmaceutical industry.[1, 2] The interest relies on the fact that co-crystals are potentially different in physical and chemical properties (solubility and intrinsic dissolution rate, melting point, colour, etc.) from their co-formers. Moreover the co-crystallization process does not affect the chemical integrity of the molecules themselves, which is of extreme importance in the case of active pharmaceutical ingredients (APIs). From the scientific point of view the research on co-crystals and coordination networks yields new information on molecular recognition, assembly and packing.

We have reported a new class of *ionic co-crystals* (ICCs) formed by an organic molecule and an inorganic salt, such as an alkali or alkaline earth halide: in this kind of compounds the organic molecule, which is solid as a pure compound at room conditions, acts as a sort of solvating molecule towards the ions.[3-6] However the organic molecules alone cannot fulfill the request of ligands around the metals and water molecules are fundamental to complete the coordination sphere. Most of the ICCs observed so far are hydrates, which is not surprising since it is known that the presence of ionic moieties favors the formation of hydrates as already observed for the pharmaceutical salts.[7] Alkaline earth metals show an high propensity to form salts with different degree of hydration (for example $CaCl_2$ is sold as anhydrous, dehydrate, hexahydrate and it is deliquescent if left in air). This behavior is observed also for calcium based organic salts see for example the pigment red 57:1 which presents three degree of hydration corresponding to three different colors.[8] Great efforts have been made to establish the hydrate stability depending on the moister condition because it is known that APIs can convert into different hydrated forms depending on the relative humidity (RH%),[9-13] as phases with different hydration states generally exhibit different physical properties, such as dissolution rate and bioavailability, which can affect product performances.[14-16] It is worth noting that the RH% can be quite different depending on latitude, longitude and period of the year: in the USA alone the average RH range is wide, leading to figures of 75.9% in New Orleans or just 30% in Las Vegas.

Nicotinamide, also known as niacimide, is a vitamin from the vitamin B group with a recommended daily allowance of 0.3 mg kg^{-1} day^{-1} and its deficiency causes pellagra in humans.[17] In the last decade epidemiological studies suggest a role of vitamins and minerals assumed with fruits and vegetables, as well as essential fatty acids in protection against disease[18] and several studies has been done on nicotinamide as candidate in neuroprotection.[19-21] Moreover it has been observed that the combination of nicotinamide together with calcium carbonate reduce the hyperphosphatemia in patients undergoing haemodialysis.[22]

Several nicotinamide co-crystals have been published[23-50] and among them the ICCs of nicotinamide (an API) with $CaCl_2$.[4] The intrinsic dissolution rate and the thermal behaviour of the nicotinamide·$CaCl_2$·H_2O (**Nic·$CaCl_2$·H_2O**) and nicotinamide$_2$·$CaCl_2$·$2H_2O$ (**Nic$_2$·$CaCl_2$·$2H_2O$**) were studied and compared with those of the pure organic co-former; in particular the thermal stability is highly increased: while pure nicotinamide melts at 132 °C, **Nic·CaCl$_2$·H$_2$O** is stable up to 240 °C. These features prompted us to study this system further, in order to establish all the possible hydrated forms and their stability. In this sense monitoring and controlling the hydration state of active pharmaceutical compounds as a function of temperature and relative humidity is crucial in order to ensure a certain stability for drug products.[51] Moreover post-synthesis (de)hydration can lead to new phases which cannot be obtained as first product for kinetic or thermodynamic reasons. The transformation of one hydrated form to the other generally yields a powder product with no suitable crystallite for single crystal diffraction. Thus, in order to fully characterize the new unknown phase, it is of extreme importance to obtain a pure phase by adjusting the physical and chemical conditions.

Here we report our results for the preparation and characterization of the hydration states of the ICC of nicotinamide with $CaCl_2$ by solid state controlled humidity method, and its behaviour with temperature. Two new crystal forms were solved from powder diffraction. Crystalline products were analysed with DSC, TGA and variable temperature PXRD.

Experimental Details

All reagents and solvents were purchased from Sigma-Aldrich and used without further purification.

Synthesis in Solution

$CaCl_2$ (0.1 mmol) and nicotinamide (0.1 mmol) were dissoleved in 20 mL of absolute ethanol: the solution was left to evaporate at room temperature, yielding crystalline **Nic$_2$·CaCl$_2$·2H$_2$O**.

Solid State Synthesis

Nic·CaCl$_2$·H$_2$O was obtained by ball milling (using a Retsch MM 200 Mixer Mill) nicotinamide (1 mmol) and $CaCl_2$ (1 mmol) for 120 minutes with a drop of absolute ethanol; the reaction was quantitative.

Anhydrous **Nic·CaCl$_2$** ICC was obtained by heating **Nic·CaCl$_2$·H$_2$O** at 150 °C overnight.

Controlled Humidity Experiments

The controlled relative humidity (RH) environments were achieved using supersaturated aqueous solutions of LiCl, $MgCl_2$, $Mg(NO_3)_2$, and NaCl, in sealed containers, which yielded 11, 33, 54, 75% RH, respectively. **Nic·CaCl$_2$** powder or **Nic·CaCl$_2$·H$_2$O** powder was placed in these sealed containers at room temperature. **Nic$_2$·CaCl$_2$·2H$_2$O** was obtained after two weeks in such a container with 33% or 54% RH at room temperature. **Nic·CaCl$_2$·4H$_2$O** was obtained after two weeks in such a container with 75% RH at room temperature.

X-ray Powder Diffraction

All data were collected in Bragg-Brentano geometry on a Panalytical X'Pert PRO automated diffractometer equipped with an X'Celerator detector, using Cu-Kα radiation without a monocromator.

For structure solution and refinement purposes X-ray powder diffractograms in the 2θ range 5-70° (step size 0.01°, time/step 50 s, 0.02 rad soller, kVxmA 40x40).

For phase identification purposes X-ray powder diffractograms in the 2θ range 5-40° (step size 0.02°, time/step 20 s, 0.04 rad soller, kVxmA 40x40). .

Variable Temperature X-ray Powder Diffraction

The data were collected in open air in Bragg-Brentano geometry using Cu-Kα radiation without a monocromator. X-ray powder diffractograms in the 2θ range 5-50° were collected on a Panalytical X'Pert PRO automated diffractometer equipped with an X'Celerator detector and an Anton Paar TTK 450 system for measurements at controlled temperature.

Thermogravimetric Analysis (TGA)

TGA measurements were performed using a Perkin Elmer TGA7 in the temperature range 30-400 °C under N_2 gas flow, at a heating rate of 5 °C min^{-1}.

Structure of Nic·CaCl$_2$

Powder diffraction data were analyzed with the software DASH.[52] The anhydrous phase is known to convert into the monohydrated ICC in a matter of hours, and the major peaks of **Nic·CaCl$_2$·H$_2$O** at ~10.5°, ~15° and 17.7° were indeed present in the powder pattern. Thus 21 peaks were carefully chosen in the 2θ range 5-40° and a monoclinic cell was found with a volume of 486 Å^3 using the algorithm DICVOL.[53] Such volume is compatible with the presence of 2 nicotinamide·$CaCl_2$ formula units. Space group determination with DASH resulted in space group nr. 7, *i.e. Pn*, with multiplicity 2 and Z' = 1. The crystal structure was solved by simulated annealing using one nicotinamide molecule, one Ca^{2+} ion, and two chloride ions. 25 runs were performed with 10^7 maximum number of moves each. The best solution was chosen for Rietveld refinement. Rietveld refinement was performed with the software TOPAS.[54] **Nic·CaCl$_2$·H$_2$O** phase was inserted in the refinement together with the starting structural model for the anhydrous phase. A shifted Chebyshev function with 12 parameters and a Pseudo-Voigt function (TCHZ type) were used to fit background and peak shape, respectively. Restraints on bond distances and angles of nicotinamide molecule were applied after an initial rigid body approach. A spherical harmonics model was used to describe preferred orientation. Only the scale factor, the cell parameters, the peak shape and no structural parameter were refined for **Nic·CaCl$_2$·H$_2$O** instead. Refinement converged to cell parameters a = 18.1964(7) Å, b = 8.1426(3) Å, c = 3.9569(1) Å, β = 124.043(2) ° with χ^2 = 1.222, R_{wp} = 8.48%, R_B = 2.84% (CCDC deposition number 990169).

The amount of the **Nic·CaCl$_2$·H$_2$O** was assessed to 5.7%. The Rietveld refinement plot is shown in Figure 1.

Cite this: DOI: 10.1039/c0xx00000x

www.rsc.org/xxxxxx

ARTICLE TYPE

Table 1. Crystallographic details for all ICCs of nicotinamide and $CaCl_2$.

	Nic·CaCl$_2$†	**Nic·CaCl$_2$·H$_2$O‡**	**Nic$_2$·CaCl$_2$·2H$_2$O‡**	**Nic·CaCl$_2$·4H$_2$O†**
chemical formula	$C_6H_6CaCl_2N_2O$	$C_6H_8CaCl_2N_2O_2$	$C_{12}H_{16}CaCl_2N_4O_4$	$C_6H_{14}CaCl_2N_2O_5$
crystal system	monoclinic	triclinic	monoclinic	orthorhombic
space group	*P n*	*P -1*	*C 2/c*	*P n a 2$_1$*
Z	2	2	4	4
a **(Å)**	18.1964(7)	9.6884(2)	21.740(1)	17.5215(6)
b **(Å)**	8.1426(3)	9.2781(1)	6.872(3)	11.4158(4)
c **(Å)**	3.9569(1)	6.1967(1)	12.8167(7)	6.7943(2)
α (º)	90	103.3036(2)	90	90
β (º)	124.043(2)	98.564(1)	117.775(7)	90
γ (º)	90	107.858(2)	90	90
V **(Å^3)**	485.79(3)	502.027(8)	1694.1(2)	1359.00(8)

† this work; ‡ Braga et al. (2012) [4]

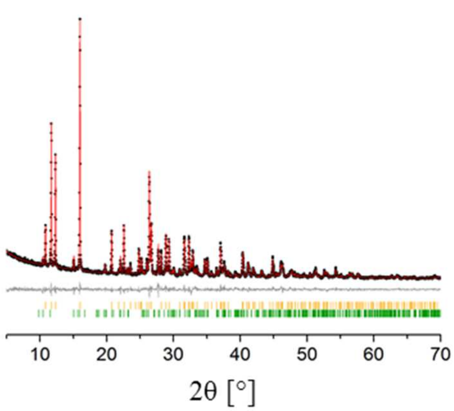

Fig. 1 Experimental (black dots), calculated (red line) and difference (grey line) patterns for **Nic·CaCl$_2$**. Peak positions are marked in orange and green for **Nic·CaCl$_2$** and **Nic·CaCl$_2$·H$_2$O** respectively.

Structure of Nic·CaCl$_2$·4H$_2$O

Powder diffraction data were analyzed with the software DASH.[52] 19 peaks were chosen in the 2θ range 5-40°, and an orthorhombic cell was found with a volume of 1355 Å^3 using the algorithm DICVOL.[53] Such volume is compatible with the presence of 4 nicotinamide·$CaCl_2$ moieties plus 16 water molecules, *i.e.* 4 times **Nic·CaCl$_2$·4H$_2$O**. TGA confirmed the water molecules to be four to five per nicotinamide·$CaCl_2$ formula unit. Space group determination with DASH resulted in space group nr. 62, *i.e. Pnam*, with multiplicity 8 and Z' = 0.5. In order to avoid special positions the $P2_12_12_1$ subgroup was used for structure solution. Following a rigid fragments approach[6] the crystal structure was solved by simulated annealing using one nicotinamide molecule, one $[Ca(O_{water})_2]^{2+}$ rigid fragment, two chloride ions and two water molecules. 25 runs were performed with 10^7 maximum number of moves each. The best solution was chosen for Rietveld refinement. Rietveld refinement was performed with the software TOPAS.[54] A shifted Chebyshev function with 12 parameters and a Pseudo-Voigt function (TCHZ type) were used to fit background and peak shape, respectively. A spherical harmonics model was used to describe preferred orientation. Restraints on bond distances and angles of nicotinamide molecule were applied after an initial rigid body approach. An overall thermal parameter for the whole nicotinamide molecule was adopted. The refinement was found to be more stable using $Pna2_1$, the non centrosymmetric subgroup of *Pnam*. Refinement converged to cell parameters a = 17.5215(6) Å, b = 11.4158(4) Å, c = 6.7943(2) Å with χ^2 = 1.460, R_{wp} = 7.53%, R_B = 3.12% (CCDC deposition number 990170). The final difference Fourier map showed no significant peak indicating the presence of any additional water molecule. Figure 2 shows the final Rietveld plot.

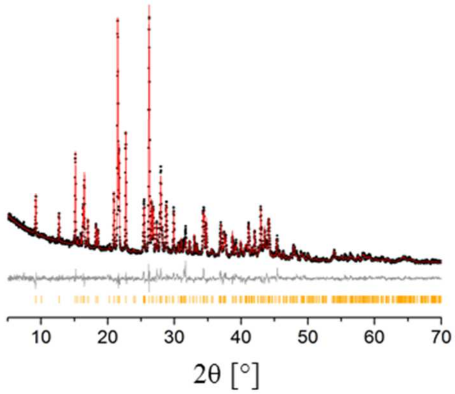

Fig. 2 Experimental (black dots), calculated (red line) and difference (grey line) patterns for **Nic·CaCl$_2$·4H$_2$O**. Peak positions are marked in orange.

Results and Discussion

Table 1 reports the crystallographic details for all the ICCs of calcium and nicotinamide. In all of these compounds the organic molecule acts as a kind of "solvent molecule" towards calcium chloride. The C=O dipoles always form electrostatic interactions with the calcium cations. Heterocyclic nitrogens, chloride anions and water molecules are competing to complete the coordination sphere of the calcium polyhedral. The N-H dipoles form hydrogen bonds with the chloride anions instead.

In **Nic·CaCl$_2$** the calcium distorted octahedron coordination involves the carbonyl group and the heterocyclic nitrogen of nicotinamide plus four chloride atoms. The framework is based on chains of calcium polyhedra sharing Cl-Cl edges and the nicotinamide molecules bridge the chains and form a bidimensional networks (Figure 3).

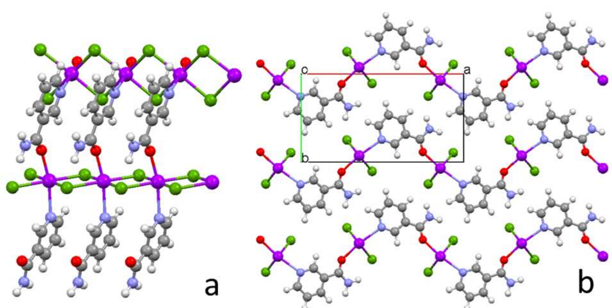

Fig. 3 Packing patterns for **Nic·CaCl$_2$** a) the coordination of the calcium ions. b) the packing view along *c*-axis. Calcium is purple, chloride is green, oxygen is red, nitrogen is light blue, carbon is grey.

As already reported,[4] in **Nic·CaCl$_2$·H$_2$O**, the calcium coordination involves the nicotinamide heterocyclic nitrogen and the carbonyl group, while one of the four chloride atoms is replaced by the oxygen of a molecule of water of hydration. The presence of this water molecule in the calcium coordination sphere lower the dimensionality of the network and it can be described by infinite ribbons (Figure 4).

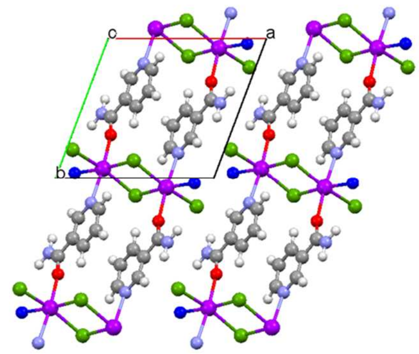

Fig. 4 Packing patterns for **Nic·CaCl$_2$·H$_2$O,** view along the *c*-axis. The oxygen of the water molecule is in blue; the hydrogen positions of the water molecule are not determinate. Calcium is purple, chloride is green, oxygen is red, nitrogen is light blue carbon is gray.

In the tetrahydrated form, due to the high number of water molecules available, the calcium coordination polyhedron involves one chloride, four water molecules, and only one nicotinamide molecule through C=O moiety. Thus in the case of nicotinamide ICCs with CaCl$_2$ water is more favored than the heterocyclic nitrogen in coordinating calcium. The calcium polyhedra are isolated in this structure, which is stabilised by hydrogen bonds. Indeed one chloride atom is involved only in hydrogen bonds (Figure 5). As previously reported the role of hydrogen bonds between neutral molecules and chloride ions is just as important as calcium coordination, and the resulting structures show no voids and large packing coefficients.[4]

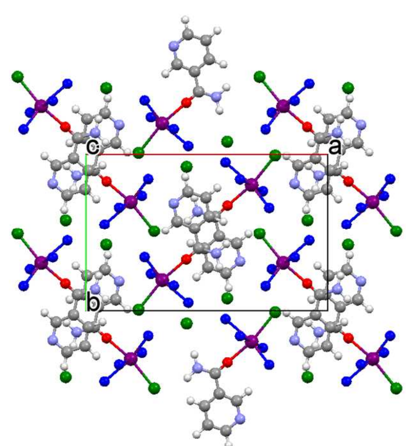

Fig. 5 Packing patterns for **Nic·CaCl$_2$·4H$_2$O,** view along the *c*-axis. The oxygen of the water molecules are in blue; the hydrogen positions of the water molecule are not determinate. Calcium is purple, chloride is green, oxygen is red, nitrogen is light blue, carbon is grey.

In order to study the stability of the four nicotinamide·CaCl$_2$ ICCs as a function of humidity, several controlled humidity batches were set. Controlled humidity was found to be crucial for the selection of the hydrated form. In particular as reported in the experimental details, a pure **Nic·CaCl$_2$·4H$_2$O** powder was obtained by keeping **Nic·CaCl$_2$** or **Nic·CaCl$_2$·H$_2$O** at 75% RH for a week. This pure product was then used to solve and refine the crystal structure of the tetra-hydrated ICC, as reported in the previous section.

The stability of the anhydrous **Nic·CaCl$_2$** has been tested at different relative humidity environments. The anhydrous phase **Nic·CaCl$_2$** was estimated to be more than 80 wt% from the Rietveld analysis after two weeks at 12%RH (see SI), while a full transformation to **Nic·CaCl$_2$·H$_2$O** was found to happen in a few hours at higher RH values. The powder pattern is shown in Figure 7 together with the calculated patterns for the anhydrous and monohydrated phases for comparison.

It was previously reported that **Nic$_2$·CaCl$_2$·2H$_2$O** only crystallizes from solution, and that dry grinding of nicotinamide with calcium chloride yields the monohydrated form.[4] Our new evidences show that the dihydrated form can be obtained by placing either **Nic·CaCl$_2$** or **Nic·CaCl$_2$·H$_2$O** at 33% - 54% RH for two weeks. Minor quantities (<10 wt%) of $CaCl_2{\cdot}4H_2O$ and $CaCl_2{\cdot}2H_2O$ were detected in the powder pattern (see SI). The powder pattern is shown in Figure 7 together with the calculated pattern for the dihydrated phase for comparison. It is worth noting that the powder was found to be very hygroscopic, as already reported in our previous article, which prevents to perform a TGA.[4] This also makes quantification by X-ray diffraction not reliable due to difficulties sampling the deliquescent wet powder and intrinsic problems when quantifying amorphous contents in general.

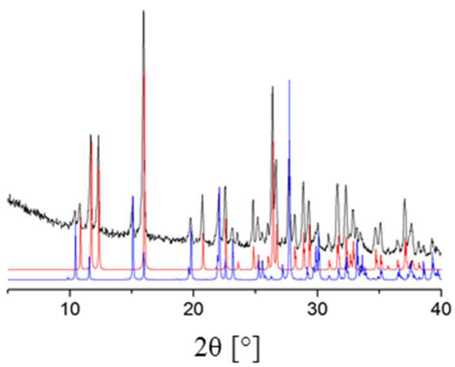

Fig. 6 Experimental powder pattern of **Nic·CaCl$_2$·H$_2$O** (black line) after two weeks at 12% RH; the calculated patterns for **Nic·CaCl$_2$** (red line) and **Nic·CaCl$_2$·H$_2$O** (blue line) are shown for comparison.

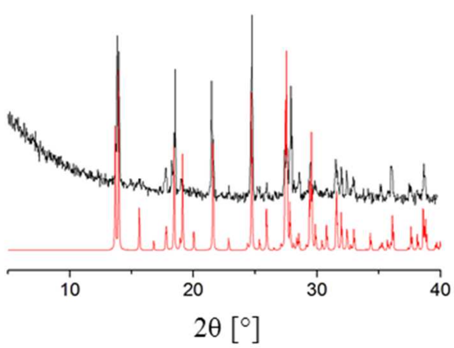

Fig. 7 Experimental powder pattern of **Nic·CaCl$_2$·H$_2$O** (black line) after two weeks at 54% RH; the calculated pattern for **Nic$_2$·CaCl$_2$·2H$_2$O** (red line) is shown for comparison.

The thermal stability of the different phases was further clarified by a weight loss of about 21% in the range 30–90 °C, which corresponds to a release of 3 molecules of water plus some adsorbed water. The water loss corresponds to the transformation of the tetrahydrate form into the monohydrate, as detected by VT-XRD data. No traces of the dehydrated form were detected. Finally the water loss process ranging from 150 °C to 200 °C corresponds to the complete dehydration to **Nic·CaCl$_2$**. The experimental XRD patterns at room temperature, 90 °C, and 200 °C summarize the results of this variable temperature study (Figure 8).

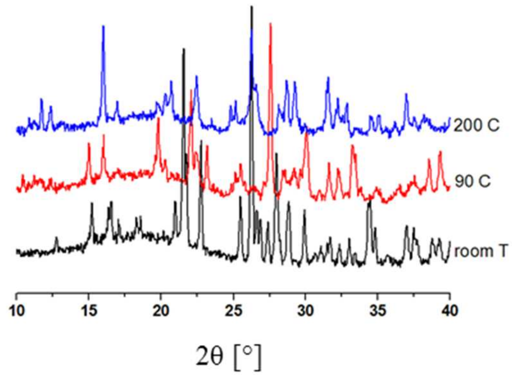

Fig. 8 Variable temperature XRD of **Nic·CaCl$_2$·4H$_2$O**: room T (black curve, **Nic·CaCl$_2$·4H$_2$O**), 90 °C (red curve, **Nic·CaCl$_2$·H$_2$O**) and 200 °C (blue curve, **Nic·CaCl$_2$**)

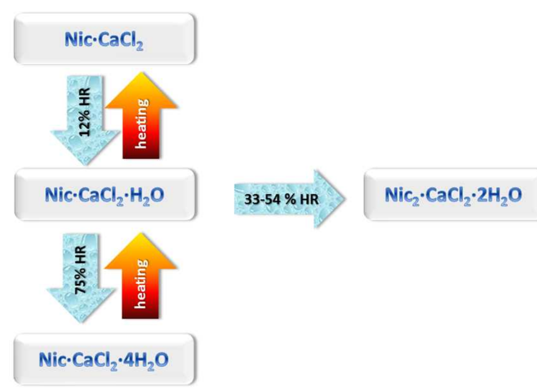

Scheme 1 The relationships between the various crystal forms of ICC based on nicotinamide and $CaCl_2$.

Conclusions

The results prove that humidity is a crucial factor for ICCs, and that exploring different RH conditions can be of extreme importance for a complete polymorph screening of this class of compounds and for industrial applications of active pharmaceutical ingredient compounds in general. The relationships between the various forms of the ionic co-crystals based on nicotinamide and $CaCl_2$ in function of the relative humidity are reported in scheme 1. The anhydrous **Nic·CaCl$_2$** converts into **Nic·CaCl$_2$·H$_2$O** at low HR% (12%), otherwise at HR > 54% it directly converts into **Nic·CaCl$_2$·4H$_2$O.** These conversions are reversible upon heating of the samples. The **Nic·CaCl$_2$·H$_2$O** and **Nic·CaCl$_2$** transforms into **Nic$_2$·CaCl$_2$·2H$_2$O** at HR 33 and 54%. The calcium chloride obtained is present in the resultant powder as $CaCl_2 \cdot 4H_2O$ and $CaCl_2 \cdot 2H_2O$, moreover the deliquescent nature of the calcium chloride salts prevented an exhaustive characterization. To conclude, phase selection and purification was achieved by controlling the relative humidity. More importantly, post-synthesis product purification was fundamental in order to solve the crystal structures for those phases that could not be obtained as single crystals. The crystal structures of two new ICC of nicotinamide and $CaCl_2$, the anhydrous and the tetrahydrated forms respectively, were solved by simulated annealing with powder diffraction data. Calcium coordination in nicotinamide·$CaCl_2$, involves also the nicotinamide heterocyclic nitrogen for one of the two nicotinamide molecules, showing that ICC systems are not confined to C=O···Ca interactions only, just as previously reported for the monohydrated form. To our knowledge, the solvation properties of molecules characterized by different kinds of dipoles such as aromatic heterocyclic nitrogens have not been systematically explored. This may open new perspectives for this class of compounds in the near future.

Notes and references

[a] *Dipartimento di Chimica "G. Ciamician", Università di Bologna, via Selmi 2 - 40126 Bologna, Italy. Fax: +39 051 2099456; E-mail: l.maini@unibo.it*
[b] *Department of Earth Sciences, University of Cambridge, Downing St - CB2 3EQ, Cambridge, UK. E-mail: gil21@cam.ac.uk*
[c] *Dipartimento di Geoscienze, Università di Padova, Via Gradenigo 6, 35131 Padova, Italy.*
[d] *EaStCHEM School of Chemistry, University of St. Andrews, Purdie Building, North Haugh, St. Andrews, Fife KY16 9ST, UK.*
† Electronic Supplementary Information (ESI) available: CCDC reference numbers XXXXX. For ESI and crystallographic data in CIF see DOI: 10.1039/b000000x/

1. N. Schultheiss and A. Newman, *Cryst. Grow. Des.*, 2009, **9**, 2950-2967.
2. P. Vishweshwar, J. A. McMahon, M. L. Peterson, M. B. Hickey, T. R. Shattock and M. J. Zaworotko, *Chem.Commun.*, 2005, 4601-4603.
3. D. Braga, F. Grepioni, L. Maini, S. Prosperi, R. Gobetto and M. R. Chierotti, *Chem.Commun.*, 2010, **46**, 7715-7717.
4. D. Braga, F. Grepioni, G. I. Lampronti, L. Maini and A. Turrina, *Cryst. Grow. Des.*, 2011, **11**, 5621-5627.
5. D. Braga, F. Grepioni, L. Maini, D. Capucci, S. Nanna, J. Wouters, L. Aerts and L. Quere, *Chem.Commun.*, 2012, **48**, 8219-8221.
6. D. Braga, F. Grepioni, L. Maini, G. I. Lampronti, D. Capucci and C. Cuocci, *CrystEngComm*, 2012, **14**, 3521-3527.
7. U. J. Griesser, in *Polymorphism*, ed. R. Hilfiker, Wiley-VCH, Weinheim, 2006, pp. 211-233.
8. S. L. Bekö, S. M. Hammer and M. U. Schmidt, *Angew. Chem. Int. Ed.*, 2012, **51**, 4735-4738.
9. K. K. Arora, S. Thakral and R. Suryanarayanan, *Pharm. Res.*, 2013, **30**, 1779-1789.
10. M. F. Pina, J. F. Pinto, J. J. Sousa, L. Fabian, M. Zhao and D. Q. M. Craig, *Mol. Pharmaceutics*, 2012, **9**, 3515-3525.
11. V. V. Chernyshev, A. V. Yatsenko, S. V. Pirogov, T. F. Nikulenkova, E. V. Tumanova, I. S. Lonin, K. A. Paseshnichenko, A. V. Mironov and Y. A. Velikodny, *Cryst. Grow. Des.*, 2012, **12**, 6118-6125.
12. M. P. Feth, J. Jurascheck, M. Spitzenberg, J. Dillenz, G. Bertele and H. Stark, *J. Pharm. Sci.*, 2011, **100**, 1080-1092.
13. D. Braga, F. Grepioni, L. Chelazzi, M. Campana, D. Confortini and G. C. Viscomi, *CrystEngComm*, 2012, **14**, 6404-6411.
14. S. Debnath and R. Suryanarayanan, *AAPS PharmSciTech*, 2004, **5**, 39-49.
15. R. K. Khankari and D. J. W. Grant, *Thermochim. Acta*, 1995, **248**, 61-79.
16. L. Malaj, R. Censi, Z. Gashi and P. Di Martino, *Int. J. Pharm.*, 2010, **390**, 142-149.
17. M. Knip, I. F. Douek, W. P. T. Moore, H. A. Gillmor, A. E. M. McLean, P. J. Bingley and E. A. M. Gale, *Diabetologia*, 2000, **43**, 1337-1345.
18. A. Virmani, L. Pinto, Z. Binienda and S. Ali, *Molecular Neurobiology*, 2013, **48**, 353-362.
19. U. N. Das, *PLoS Med.*, 2006, **3**, 699-700.
20. T. Kristian, I. Balan, R. Schuh and M. Onken, *J. Neurosci. Res.*, 2011, **89**, 1946-1955.
21. Y. Ma, H. Chen, X. He, H. Nie, Y. Hong, C. Sheng, Q. Wang, W. Xia and W. Ying, *Curr. Drug Targets*, 2012, **13**, 222-229.
22. S. Allam, M. El-Hamamsy and M. El Sharkawy, *Advances in Natural Science*, 2012, **5**, 1-9.
23. D. J. Berry, C. C. Seaton, W. Clegg, R. W. Harrington, S. J. Coles, P. N. Horton, M. B. Hursthouse, R. Storey, W. Jones, T. Friscic and N. Blagden, *Cryst. Grow. Des.*, 2008, **8**, 1697-1712.
24. S. Nicoli, S. Bilzi, P. Santi, M. R. Caira, J. Li and R. Bettini, *J. Pharm. Sci.*, 2008, **97**, 4830-4839.
25. N. Chieng, M. Hubert, D. Saville, T. Rades and J. Aaltonen, *Cryst. Grow. Des.*, 2009, **9**, 2377-2386.
26. J. Lu and S. Rohani, *Org. Process Res. Dev.*, 2009, **13**, 1269-1275.
27. J. I. Arenas-Garcia, D. Herrera-Ruiz, K. Mondragon-Vasquez, H. Morales-Rojas and H. Hopfl, *Cryst. Grow. Des.*, 2010, **10**, 3732-3742.
28. L. J. Thompson, R. S. Voguri, A. Cowell, L. Male and M. Tremayne, *Acta Crystallogr. Sect. C-Cryst. Struct. Commun.*, 2010, **66**, o421-o424.
29. A. Lemmerer, C. Esterhuysen and J. Bernstein, *J. Pharm. Sci.*, 2010, **99**, 4054-4071.
30. S. Boyd, K. Back, K. Chadwick, R. J. Davey and C. C. Seaton, *J. Pharm. Sci.*, 2010, **99**, 3779-3786.
31. T. Kojima, S. Tsutsumi, K. Yamamoto, Y. Ikeda and T. Moriwaki, *Int. J. Pharm.*, 2010, **399**, 52-59.
32. N. B. Bathori, A. Lemmerer, G. A. Venter, S. A. Bourne and M. R. Caira, *Cryst. Grow. Des.*, 2011, **11**, 75-87.
33. L. Fabian, N. Hamill, K. S. Eccles, H. A. Moynihan, A. R. Maguire, L. McCausland and S. E. Lawrence, *Cryst. Grow. Des.*, 2011, **11**, 3522-3528.
34. B. Lou and S. Hu, *Journal of Chemical Crystallography*, 2011, **41**, 1663-1668.
35. B. Das and J. B. Baruah, *Cryst. Grow. Des.*, 2011, **11**, 5522-5532.
36. R. A. E. Castro, J. D. B. Ribeiro, T. M. R. Maria, M. Ramos Silva, C. Yuste-Vivas, J. Canotilho and M. E. S. Eusebio, *Cryst. Grow. Des.*, 2011, **11**, 5396-5404.

37. F. N. F. How, M. S. Amalina, H. Khaledi and H. M. Ali, *Acta Crystallographica Section E-Structure Reports Online*, 2011, **67**, O3168-U3173.
38. T. Ueto, N. Takata, N. Muroyama, A. Nedu, A. Sasaki, S. Tanida and K. Terada, *Cryst. Grow. Des.*, 2012, **12**, 485-494.
39. A. Alhalaweh, S. George, S. Basavoju, S. L. Childs, S. A. A. Rizvi and S. P. Velaga, *CrystEngComm*, 2012, **14**, 5078-5088.
40. K. Maruyoshi, D. Iuga, O. N. Antzutkin, A. Alhalaweh, S. P. Velagad and S. P. Brown, *Chem.Commun.*, 2012, **48**, 10844-10846.
41. S. Aitipamula, A. B. H. Wong, P. S. Chow and R. B. H. Tan, *CrystEngComm*, 2012, **14**, 8193-8198.
42. N. R. Goud, S. Gangavaram, K. Suresh, S. Pal, S. G. Manjunatha, S. Nambiar and A. Nangia, *J. Pharm. Sci.*, 2012, **101**, 664-680.
43. S.-W. Zhang, I. A. Guzei, M. M. de Villiers, L. Yu and J. F. Krzyzaniak, *Cryst. Grow. Des.*, 2012, **12**, 4090-4097.
44. P. Sanphui, S. S. Kumar and A. Nangia, *Cryst. Grow. Des.*, 2012, **12**, 4588-4599.
45. Y. Gao, J. Gao, Z. Liu, H. Kan, H. Zu, W. Sun, J. Zhang and S. Qian, *Int. J. Pharm.*, 2012, **438**, 327-335.
46. S. Jin, D. Wang, Q. Linhe, M. Fu, S. Wu and J. Ren, *Journal of Chemical Crystallography*, 2013, **43**, 258-265.
47. H. M. Ratajczak, I. Bryndal, I. Ledoux-Rak and A. J. Barnes, *J. Mol. Struct.*, 2013, **1047**, 310-316.
48. I. Tomaszewska, S. Karki, J. Shur, R. Price and N. Fotaki, *Int. J. Pharm.*, 2013, **453**, 380-388.
49. M. Sowa, K. Slepokura and E. Matczak-Jon, *Acta Crystallogr. Sect. C-Cryst. Struct. Commun.*, 2013, **69**, 1267-U1291.
50. S.-W. Zhang, M. T. Harasimowicz, M. M. de Villiers and L. Yu, *J. Am. Chem. Soc.*, 2013, **135**, 18981-18989.
51. D. Raijada, A. D. Bond, F. H. Larsen, C. Cornett, H. Qu and J. Rantanen, *Pharm. Res.*, 2013, **30**, 280-289.
52. W. I. F. David, K. Shankland, J. van de Streek, E. Pidcock, W. D. S. Motherwell and J. C. Cole, *J. Appl. Crystallogr.*, 2006, **39**, 910-915.
53. A. Boultif and D. Louer, *J. Appl. Crystallogr.*, 2004, **37**, 724-731.
54. A. Cohelo, *TOPAS-Academic*, (2007) Coelho Software, Brisbane, Australia.

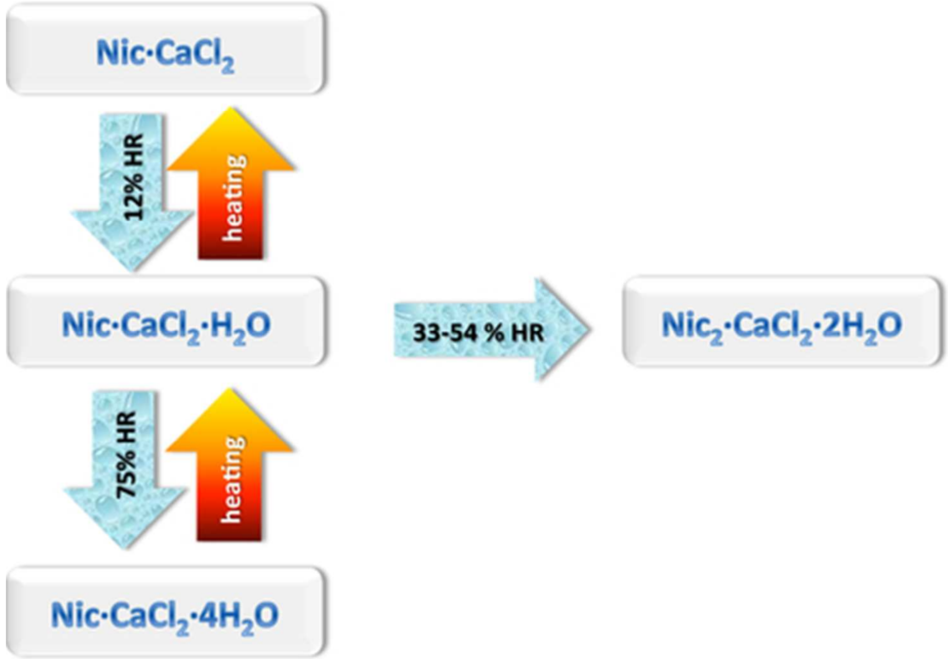

39x27mm (300 x 300 DPI)